Available online at www.sciencedirect.com
ScienceDirect
Ceramics International 35 (2009) 661–664
CERAMICS INTERNATIONAL
www.elsevier.com/locate/ceramint

Preparation of spherical nanoparticles of $LaAlO_3$ via the reverse microemulsion process

Zhongqing Tian *, Weijiu Huang, Yijing Liang

School of Materials Science and Engineering, Chongqing Institute of Technology, 4 Xingsheng Road, Chongqing 400050, PR China

Received 25 September 2007; received in revised form 6 October 2007; accepted 28 January 2008
Available online 23 April 2008

Abstract

Spherical $LaAlO_3$ nanoparticles in a reverse microemulsion consisting of solution (water phase), Tween-80 and Span-80 (surfactant), *n*-butanol (cosurfactant, and cyclohexane (oil phase) were prepared. Precursor powders and calcined powders were characterized by differential thermal analysis (DTA), thermogravimetry analysis (TG), X-ray diffraction (XRD) and transmission electron microscopy (TEM). A pure perovskite $LaAlO_3$ formed when the precursor hydroxides calcined at 800 °C for 2 h. The particle size was about 50 nm and the shape of the monodisperse particles is spherical. The reverse microemulsion process can dramatically lower the crystallization temperature of $LaAlO_3$ about 700 °C than the classical solid-state reaction method.
© 2008 Elsevier Ltd and Techna Group S.r.l. All rights reserved.

Keywords: Microemulsion; Synthesis; Nanoparticles; $LaAlO_3$

1. Introduction

Lanthanum aluminate ($LaAlO_3$) were widely used as the substrates of high-temperature superconductor and ferroelectric thin films due to their low dielectric loss and minor lattice parameter mismatch between the substrates and film [1–2]. $LaAlO_3$ ceramics are also potential microwave dielectric materials because of their high Q_f value (68,000 GHz) and relative low temperature coefficient of resonant frequency τ_f (−44 ppm/°C) [3]. Due to its high surface area and catalytic activity, $LaAlO_3$ has also been used as catalyst for oxidative coupling of methane and hydrogenation and hydrogenolysis of hydrocarbons [4]. Its preparation by the classical solid-state reaction requires a high calcination temperature (1500–1700 °C) and hence induces the sintering and aggregation of particles [5–8]. Although there have been a number of reports demonstrating the achievements in wet chemically preparing the $LaAlO_3$ nanoparticles through kinds of approaches such as sol–gel [9,10], co-precipitation [11,12], aerosol-furnace technique [13], TEA gel route [14] and combustion method [15], it is still worth improving the particles morphology and enhancing the crystallinity at a low calcination temperature. In recent years, microemulsion method has been studied and utilized widely and has been a key technique to synthesize oxide nanoparticles owing to the products which has a characteristic of well dispersed, controlled size and narrow size distribution [16–18]. However, the synthesis of lanthanum aluminate has been rarely reported by the microemulsion technology. In this work, a reverse microemulsion process was used to prepare spherical nanoparticles of $LaAlO_3$ at low calcination temperature.

2. Experimental

The starting materials include NH_4OH, $Al(NO_3)_3{\cdot}9H_2O$ and $La(NO_3)_3{\cdot}6H_2O$, Span-80, Tween-80, cyclohexane, *n*-butanol. All chemical reagents were of analytic purity. The flow chart for preparing $LaAlO_3$ nanoparticles by the reverse microemulsion process is shown in Fig. 1. Firstly, 20 g of 0.3 mol/L $Al(NO_3)_3 + La(NO_3)_3$ solution was dissolved in 26.7 g mixture of Span-80 and Tween-80 (the ratio is 0.667), 13.3 g *n*-butanol, 40 g cyclohexane mixed solvent with vigorous stirring till the system was formed a transparent microemulsion. In the same way, 20 g of 2 mol/L ammonia water was added in the same mixed solvent to form a transparent system. Subsequently, two kinds of microemulsions were mixed together with a

* Corresponding author. Tel.: +86 23 68666425; fax: +86 23 68668484.
E-mail address: tzqmail@sohu.com (Z. Tian).

0272-8842/$34.00 © 2008 Elsevier Ltd and Techna Group S.r.l. All rights reserved.
doi:10.1016/j.ceramint.2008.01.020

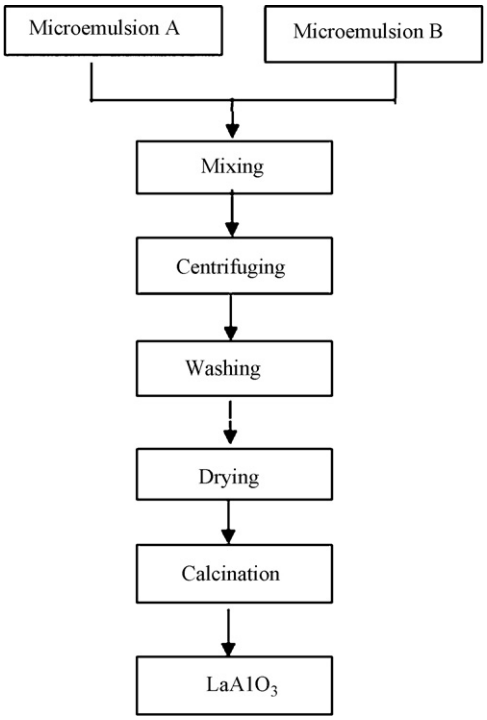

Fig. 1. Flow chart for preparing $LaAlO_3$ nanoparticles by the reverse microemulsion process (Microemulsion A: Tween-80 + Span-80/*n*-butanol/cyclohexane/$La(NO_3)_3$ + $Al(NO_3)_3$ solution; Microemulsion B: Tween-80 + Span-80/*n*-butanol/cyclohexane/NH_4OH solution.).

continuous stirring. The system still remained clear and transparent. It may be inferred that the microemulsion structure was thus preserved and the co-precipitation reaction took place in the nanosized aqueous domains [16]. The mixed system was then centrifuged, and the hydroxide precursor was washed with deionized water and acetone alternatively for three times, and dried in a vacuum oven at 90 °C for 24 h. Then the hydroxide precursors were transferred into a muffle furnace and calcined at different temperature for 2 h.

Thermogravimetric analysis (TGA) and differential scanning calorimetry (DSC) were carried out for the hydroxide precursor at a heating rate of 10 °C/min under static air on SDT Q600 instruments. X-ray diffraction (XRD) patterns were recorded using a Rigaku X-ray diffractometer with Ni filtered CuKα radiation (0.15418 nm) to determine the phases present in the calcined powders. The crystallite size was estimated from the X-ray line broadening of the (1 1 0) diffraction peak using the Scherrer formula [19]

$$D_{\mathrm{XRD}} = \frac{0.9\lambda}{\beta\cos\theta}, \tag{1}$$

where D_{XRD} is the crystallite size in nm, λ is the radiation wavelength, θ is the diffraction peak angle and β is the corrected line width at half-peak intensity. The correction for instrumental peak broadening was made using the Warren formula: $\beta = (b_{\mathrm{obs}}^2 - b^2)^{1/2}$, where b_{obs} is the line width at half-peak intensity related to $LaAlO_3$ powder and b is the line width of the (1 1 0) diffraction peak of the $LaAlO_3$ sintered at 1500 °C for 12 h. The specific surface area of the powder was measured by the BET technique with nitrogen. The particle size was calculated from the data of specific surface area, by the equation

$$D_{\mathrm{BET}} = \frac{6}{\rho S} \tag{2}$$

where D_{BET} is the average diameter of a spherical particle; S, the surface area of a powder; and ρ, the theoretical density of $LaAlO_3$ (5860 kg m^{-3}). The shape and size of $LaAlO_3$ particles were observed by transmission electron microscopy (TEM: Hitachi 7500).

3. Results and discussions

The TGA and DSC curves of the obtained hydroxide precursor are shown in Fig. 2. The DSC curve indicated that there was one exothermic peak at 479 °C and two endothermic peaks at 46 and 315 °C, respectively. The endothermic peak appears at about 46 °C which corresponds to the elimination of residual water and solvent. Previous workers [20,21] have reported $Al(OH)_3$ decomposition takes place at 300, 375 and 425 °C which finally results in Al_2O_3 formation, and $La(OH)_3$ decomposition takes place at 300 °C which finally results in La_2O_3 formation. It may be inferred that endothermic peak at 315 °C represents the decomposition of $Al(OH)_3$ and $La(OH)_3$. The exothermic peak at 479 °C may be associated with the burning of the residual surfactant/or cosurfactant. The TGA curve is in agreement with the DSC peaks showing distinct regimes of weight loss corresponding to the temperature regions mentioned in the DSC.

The XRD patterns of the obtained hydroxide precursor calcined in air at 700–1000 °C for 2 h are shown in Fig. 3. The precursor and the product after the calcination at 700 °C for 2 h was primarily amorphous in structure and no distinct crystallinity phase could be detected. Also, the absence of peaks corresponding to $Al(OH)_3$ or $La(OH)_3$ indicates the amorphous nature of the obtained hydroxide precursor. The powder calcined at 800 °C for 2 h shows good crystallinity. These XRD peaks correspond to reflections from rhombohedral $LaAlO_3$ with a perovskite structure (JCPDS card 31-0022). Further heating only increased the intensity of the X-ray peaks and no

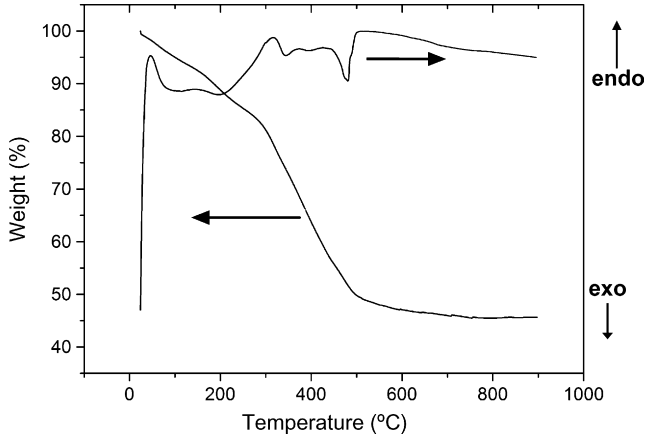

Fig. 2. TGA–DSC curves of the hydroxide precursor.

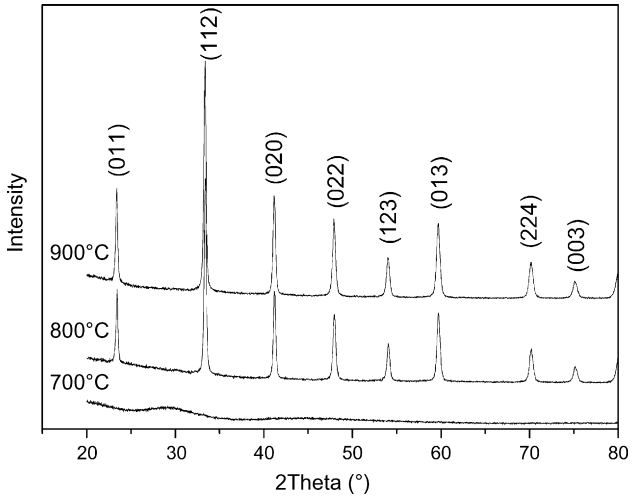

Fig. 3. X-ray patterns of the powders calcined at different temperatures for 2 h: (a) hydroxide precursor; (b) 700 °C; (c) 800 °C; (d) 900 °C; (e) 1000 °C.

other phases' peaks are observed. It is very interesting that no reflections from La_2O_3 and Al_2O_3 were observed as distinct intermediate phase prior to the formation of $LaAlO_3$ during the thermal decomposition of the powder precursor even at 700 °C. It indicates that $LaAlO_3$ maybe form through a solid-state reaction between amorphous La_2O_3 and amorphous Al_2O_3 fine particles which originated from the decomposition of $La(OH)_3$ and $Al(OH)_3$ according to TGA and DSC curves. The reaction process during the reverse microemulsion process could be described as the following equations:

$$La(NO_3)_3 + Al(NO_3)_3 + NH_4OH \rightarrow La(OH)_3 + Al(OH)_3 + NH_4NO_3 \quad (3)$$

$$La(OH)_3 + Al(OH)_3 \rightarrow \frac{1}{2}La_2O_3 + \frac{1}{2}Al_2O_3 + 3H_2O \quad (4)$$

$$\frac{1}{2}La_2O_3 + \frac{1}{2}Al_2O_3 \rightarrow LaAlO_3 \quad (5)$$

Note that the reverse microemulsion process can dramatically lower the crystallization temperature of $LaAlO_3$ about 700 °C than the classical solid-state reaction method [5–8].

Table 1 shows the variation of average crystalline size (D_{XRD}), specific surface (S) and average particle size (D_{BET}) obtained from the surface area of the powders heated at different temperatures for 2 h. The crystallite sizes calculated from the Scherrer formula are in the range of 48–75 nm. Specific surface of the $LaAlO_3$ powders calcined at different temperatures were in the range of 10.7–19 $m^2\ g^{-1}$. The average

Table 1
Variation of average crystalline size and average particle size with different calcination temperatures

Calcination temperature (°C)	D_{XRD} (nm)	S ($m^2\ g^{-1}$)	D_{BET} (nm)
800	48	19	54
900	55	16.3	63
1000	75	10.7	95

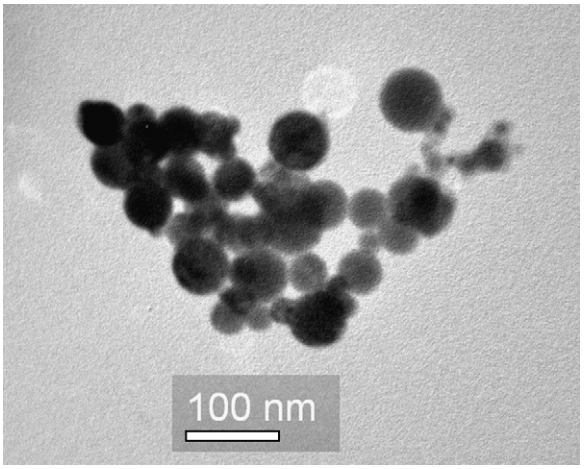

Fig. 4. TEM micrograph of $LaAlO_3$ particles calcined at 800 °C for 2 h.

particle sizes obtained from the surface area are in the range of 54–95 nm. The particle sizes calculated from surface area are comparable with the crystallite sizes calculated from XRD line broadening when calcination temperature was 800 °C. It was observed that the surface area decreases as the calcination temperature increases because of the growth and aggregation of the powders at higher temperature.

The TEM micrograph of powder calcined at 800 °C is shown in Fig. 3. From the TEM image, it can be seen that individual particles are spherical in shape with particle size of about 50 nm, which agrees very well with the result calculated from X-ray line broadening and BET value. Although the powders are calcined at 800 °C, the particles are loosely agglomerated as shown in Fig. 4.

4. Conclusion

The above studies illustrate a method to prepare spherical $LaAlO_3$ nanoparticles in a reverse microemulsion consisting of solution (water phase), Tween-80 and Span-80 (surfactant), *n*-butanol (cosurfactant, and cyclohexane (oil phase). A pure perovskite $LaAlO_3$ formed when the precursor hydroxides calcined at 800 °C for 2 h. The particle size was about 50 nm and the shape of the monodisperse particles is spherical. The reverse microemulsion process can dramatically lower the crystallization temperature of $LaAlO_3$ about 700 °C than the classical solid-state reaction method.

Acknowledgement

The work was supported by Natural Science Foundation Project of CQTC (2005BA4019).

References

[1] R.W. Simon, C.E. Platt, A.E. Lee, G.S. Lee, K.P. Daly, M.S. Wire, J.A. Luine, M. Urbanik, Low-loss substrate for epitaxial growth of high temperature superconductor thin film, Appl. Phys. Lett. 53 (1988) 2677–2679.

[2] Y. Gim, T. Hudson, Y. Fan, C. Kwon, A.T. Findikoglu, B.J. Gibbons, B.H. Park, Q.X. Jia, Microstructure and dielectric properties of $Ba_{1-x}Sr_xTiO_3$

films grown on $LaAlO_3$ substrates, Appl. Phys. Lett. 77 (2000) 1200–1202.
[3] S.Y. Cho, I.T. Kim, K.S. Hong, Microwave dielectric properties and applications of rare-earth aluminates, J. Mater. Res. 14 (1999) 114–119.
[4] R. Spinicci, P. Marini, S.D. Rossi, M. Faticanti, P. Porta, Oxidative coupling of methane on $LaAlO_3$ perovskites partially substituted with alkali or alkali-earth ions, J. Mol. Catal. A: Chem. 176 (2001) 253–265.
[5] I.A. Bonder, N.V. Vinogradona, Phase equilibrium in the lanthanum oxide-alumina system, Bull. Acad. Sci. USSR 5 (1964) 785–790.
[6] M.L. Keith, R. Roy, Structural relations among double oxides of trivalent element, Am. Mineral. 39 (1954) 1–23.
[7] G.Y. Sung, K.Y. Kang, S.C. Park, Synthesis and preparation of lanthanum aluminate target for radio-frequency magnetron sputtering, J. Am. Ceram. Soc. 74 (1991) 437–439.
[8] Q. Zhang, F. Saito, Mechanochemical synthesis of lanthanum aluminate by grinding lanthanum oxide with transition alumina, J. Am. Ceram. Soc. 83 (2000) 439–441.
[9] P. Peshev, V. Slavova, Preparation of lanthanum aluminate thin films by a sol–gel procedure using alkoxide precursors, Mater. Res. Bull. 29 (1994) 255–261.
[10] Y. Xu, G. Huang, H. Long, Synthesis of lanthanum aluminate via the ethylenediaminetetraacetic acid gel route, Ceram. Int. 29 (2003) 837–840.
[11] W. Li, M.W. Zhuo, J.L. Shi, Synthesizing nano $LaAlO_3$ powders via co-precipitation method, Mater. Lett. 58 (2004) 365–368.
[12] C.L. Kuo, C.L. Wang, T.Y. Chen, G.J. Chen, I.M. Hung, C.J. Shih, K.Z. Fung, Low temperature synthesis of nanocrystalline lanthanum monoaluminate powders by chemical coprecipitation, J. Alloys Compd. 440 (2007) 367–374.
[13] B.C. Lux, R.D. Clark, A. Salazan, L.K. Sveumand, M.A. Krebs, Aerosol generation of lanthanum aluminate, J. Am. Ceram. Soc. 76 (1993) 2669–2672.
[14] S.L. Ran, L. Gao, Synthesis of $LaAlO_3$ powder using triethanolamine, Ceram. Int. 34 (2008) 443–446.
[15] M.D.S. Kumar, T.M. Srinivasan, P. Ramasamy, C. Subramanian, Synthesis of lanthanum aluminate by a citrate-combustion route, Mater. Lett. 25 (1995) 171–174.
[16] J. Wang, P.F. Chong, S.C. Ng, L.M. Gan, Microemulsion processing of manganese zinc ferrites, Mater. Lett. 30 (1997) 217–221.
[17] W. Liu, W. Zhong, X.L. Wu, N.J. Tang, Y.W. Du, Hydrothermal microemulsion synthesis of cobalt nanorods and self-assembly into square-shaped nanostructure, J. Cryst. Growth 284 (2005) 446–452.
[18] M. Shen, Y.K. Du, P. Yang, J. Long, Morphology control of the fabricated hydrophobic gold nanostructures in W/O microemulsion under microwave irradiation, J. Phys. Chem. Solids 66 (2005) 1628–1634.
[19] H.P. Klug, L.E. Alexander, X-ray Diffraction Procedures, John Wiley and Sons, New York, 1974.
[20] S.K. Behera, P.K. Sahu, S.K. Pratihar, S. Bhattacharyya, Low temperature synthesis of spherical lanthanum aluminate nanoparticles, Mater. Lett. 58 (2004) 3710–3715.
[21] S. Bhattacharyya, S.K. Pratihar, R.K. Sinha, R.C. Behera, R.I. Ganguly, Preparation of alumina–high zirconia microcomposite by combined gel-precipitation, Mater. Lett. 53 (2002) 425–431.